

General Disclaimer

One or more of the Following Statements may affect this Document

- This document has been reproduced from the best copy furnished by the organizational source. It is being released in the interest of making available as much information as possible.
- This document may contain data, which exceeds the sheet parameters. It was furnished in this condition by the organizational source and is the best copy available.
- This document may contain tone-on-tone or color graphs, charts and/or pictures, which have been reproduced in black and white.
- This document is paginated as submitted by the original source.
- Portions of this document are not fully legible due to the historical nature of some of the material. However, it is the best reproduction available from the original submission.

(NASA-TM-87369) A NEW CLASS OF SOLAR BURST
WITH MM-WAVE EMISSION BUT ONLY AT THE
HIGHEST FREQUENCY (90 GHz) (NASA) 14 p
HC A02/MF A01

N84-35264

CSCL 03B

Unclass

G3/92 23169



SECRETARIA DE PLANEJAMENTO DA PRESIDÊNCIA DA REPÚBLICA

CONSELHO NACIONAL DE DESENVOLVIMENTO CIENTÍFICO E TECNOLÓGICO

RECEIVED BY
NASA STI FACILITY
DATE *10-25-84*
DCAF NO. *00029419*
PROCESSED BY
 NASA STI FACILITY
 ESA - SDS AIAA



INSTITUTO DE PESQUISAS ESPACIAIS

1. Publication N° INPE-3241-PRE/587	2. Version	3. Date August 1984	5. Distribution <input type="checkbox"/> Internal <input checked="" type="checkbox"/> External <input type="checkbox"/> Restricted
4. Origin DAS-DRA	Program RADIO		
6. Key words - selected by the author(s) Solar mm-wave bursts; mm-wave(only) bursts; mm-wave and hard X-ray bursts			
7. U.D.C.: 523.745			
8. Title A NEW CLASS OF SOLAR BURST WITH MM-WAVE EMISSION BUT ONLY AT THE HIGHEST FREQUENCY (90 GHz)		10. N° of pages: 13	11. Last page: 12
9. Authorship P. Kaufmann E. Correia J. E. R. Costa A. M. Zodi Vaz B. R. Dennis*		12. Revised by <i>P. Kaufmann</i> Pierre Kaufmann	13. Authorized by <i>N. Parada</i> Nelson de Jesus Parada Director General
14. Abstract/Notes - The first high sensitivity and high time resolution solar observations at 90 GHz ($\lambda = 3.3$ mm) have identified a unique impulsive burst on 21 May 1984 with emission that was more intense at this frequency than at lower frequencies. The first major time structure of the burst was over 10 times more intense at 90 GHz than at 30 GHz, 7 GHz or 2.8 GHz. Only 6 seconds later, the 30 GHz impulsive structures started to be observed but still with lower intensity than at 90 GHz. Hard X-ray time structures at energies above 25 keV were almost identical to the 90 GHz structures to better than one second. All 90 GHz major time structures consisted of trains of multiple subsecond pulses with rise times as short as 0.03 s and amplitudes large compared to the mean flux. When detectable, the 30 GHz subsecond pulses had smaller relative amplitude and were in phase with the corresponding 90 GHz pulses.			
*NASA/GSFC-LASP			
15. Remarks - Submitted to Nature. Supported partially by FINEP.			

A NEW CLASS OF SOLAR BURST WITH MM-WAVE EMISSION BUT ONLY AT THE HIGHEST
FREQUENCY (90 GHz)

P. Kaufmann*, E. Correia*, J.E.R. Costa*, A.M. Zodi Vaz* and B.R. Dennis[†]

*INPE: Instituto de Pesquisas Espaciais, C.P. 515, 12.200 - São José dos
Campos, S.P., Brazil

[†]NASA, Goddard Space Flight Center, Laboratory for Astronomy and Solar
Physics, Greenbelt, MD 20771, U.S.A.

The first high sensitivity and high time resolution solar observations at 90 GHz ($\lambda = 3.3$ mm) have identified a unique impulsive burst on 21 May 1984 with emission that was more intense at this frequency than at lower frequencies. The first major time structure of the burst was over 10 times more intense at 90 GHz than at 30 GHz, 7 GHz or 2.8 GHz. Only 6 seconds later, the 30 GHz impulsive structures started to be observed but still with lower intensity than at 90 GHz. Hard X-ray time structures at energies above 25 keV were almost identical to the 90 GHz structures to better than one second. All 90 GHz major time structures consisted of trains of multiple subsecond pulses with rise times as short as 0.03 s and amplitudes large compared to the mean flux. When detectable, the 30 GHz subsecond pulses had smaller relative amplitude and were in phase with the corresponding 90 GHz pulses.

The past knowledge of solar burst emission at shorter mm-wavelengths is based on low sensitivity data with relatively poor time resolution (Refs. 1-7).

One of the main results of these previous observations is that certain cm-mm bursts display turnover frequencies higher than 30 GHz (i.e. $\lambda < 10$ mm). One very large burst exhibited a spectral "flattening" in the range 30-71 GHz^{4,5}, which was also found for a few other events⁷. Another peculiar event has shown emission at 90 GHz ($\lambda = 3.3$ mm) and no emission reported by patrol in the microwave range⁸. More recently, 80 GHz ($\lambda = 3.75$ mm) and 92.5 GHz ($\lambda = 3.2$ mm) solar measurements were started in Japan⁹ and Switzerland¹⁰, respectively, with 10 s.f.u. sensitivity ($1 \text{ s.f.u.} = 10^{-22} \text{ W m}^{-2} \text{ Hz}^{-1}$) and 0.3 s time resolution.

The observations presented here were made with the Itapetinga 13.7m, radome-enclosed antenna, used for the first time at 90 GHz ($\lambda = 3.3$ mm) for solar measurements in May 1984. The antenna aperture efficiency at that frequency is nearly 25 percent at the zenith and decreases with elevation angle. For solar elevation angles of 60 to 10 degrees, the corresponding sensitivity in the antenna main beam ranged from 0.07 to 0.25 s.f.u. with a time constant of 1 ms. This represents an improvement of more than two orders of magnitude in sensitivity and in time resolution over all previous observations at this frequency.

Simultaneous observations were made at 30 GHz by the same antenna with a sensitivity of 0.03 s.f.u. and a time constant of 1 ms. Active regions were tracked at the position of their maximum intensity in one of the antenna beams (usually the 90 GHz beam), and the flux scales were established by assuming that the burst sources were coincident in space with the active region maximum position. Therefore, as a result of the lack of knowledge of the source location, the flux scales are uncertain but the error should not exceed 50% in the most

extreme case. The antenna half power beam size at 90 GHz was of about 80 arcsec at about 60 degrees of elevation, at the time the burst was observed, and of about 3 arcmin at 30 GHz. The two beams axis separation was of 3 arcmin. The tracking accuracy was better than 2 arcsec r.m.s. Other details of the observational setup at Itapetinga are published elsewhere¹¹. Observations were also made at 7 GHz by a patrol radio telescope using a 1.5 m antenna with a sensitivity of 3 s.f.u. and a time constant of 20 ms.

Simultaneous observations were also made with the Hard X-ray Burst Spectrometer (HXRBS) on the Solar Maximum Mission (SMM) satellite¹². A 15 channel counting rate spectrum covering the energy range from 24 to 400 keV was obtained with this instrument every 128 ms throughout the flare.

The 90 GHz impulsive burst that occurred on 21 May 1984 at 1326 UT presented the unique characteristic of emission at the shortest mm-wavelengths only. It cannot be included in any known class of solar radio bursts. Figure 1 shows the impulsive event at 90 GHz, 30 GHz, and 7 GHz and in two hard X-ray energy ranges, 24-108 keV and 108-219 keV. The mm-wave emission spectrum suggests a turnover frequency as high as or higher than 90 GHz. The negligible rise at 7 GHz of 4 s.f.u. was confirmed by data obtained at 2.8 GHz showing a < 3 s.f.u. increase at the same time¹³.

The first major impulsive component was observed at 90 GHz nearly 6 seconds before the first impulsive structure at 30 GHz. Assuming the flux scales are correct, the first structure, labelled A in Figure 1, reached about 70 s.f.u. at 90 GHz and 6 s.f.u. at 30 GHz. The second major structure (B in Figure 1) reached 56 s.f.u. at 90 GHz and 23 s.f.u. at 30 GHz, and the third structure (C) reached 24 s.f.u. at 90 GHz and 14 s.f.u. at 30 GHz. The power law spectral index α in the relation $S \propto f^\alpha$ where S is the flux density and f is the frequency is estimated from the 30 and 90 GHz fluxes to be 2.2 for the structure A, 0.8 for B and 0.5 for C.

The hard X-ray time profiles in Figure 1 show a striking similarity to the 90 GHz time profile. Features coincide to within the 128 ms time resolution of the hard X-ray observations. It is interesting to compare the relative amplitudes of structures A and B at different X-ray energies and mm-wave frequencies. For the 24-108 keV X-rays and the 30 GHz emission, structure B is more intense than structure A, whereas for the 108-219 keV X-rays and the 90 GHz emission, structure A is more intense than structure B. This suggests that the 90 GHz emission comes primarily from the higher energy electrons or at least from electrons with a harder spectrum. The power law spectral index γ in the relation $I \propto \epsilon^{-\gamma}$ where I is the X-ray flux and ϵ is the photon energy was estimated to be 3.2 for structure A, 3.8 for B, and 4.5 for C. Nearly 1 minute after structure C, a sudden increase in γ to about 5.8 corresponding to a secondary rise in the hard X-ray flux was accompanied by weak fluctuations observed at 7 GHz and 2.8 GHz¹³. This was apparently the begining of a conventional microwave burst with a peak frequency at 8-15 GHz and a peak flux of 40 s.f.u. at 8.8 GHz occurring at 13:31 UT¹⁴, some four minutes after the initial hard X-ray and 90 GHz spikes. A minor peak in the > 24 keV X-ray flux also occurred at this time but with a HXRBS counting rate of only 300 counts s^{-1} compared to 1630 counts s^{-1} at the time of the earlier, more impulsive spikes.

The high time resolution achieved in the 90 and 30 GHz observations allowed the detection of even faster intensity variations than are evident in Figure 1. All the major impulsive structures appeared as trains of several very fast peaks when plotted on an expanded time scale. Figure 2 shows an expanded plot of structure A at 90 GHz and in 24 - 219 keV X-rays. Rapid variations are clearly detected in the 90 GHz intensity with at least 13 resolved peaks in just over

two seconds. The e-folding rise time of the initial peak is ~ 0.03 s. The detection of similar rapid variations in hard X-rays was precluded in this case by the 128 ms time resolution of the observations. However, other events have been detected by HXRBS with a time resolution of 10 ms showing equally rapid fluctuations in the hard X-ray flux¹⁵. In the present case, we can see from Figure 2 that the initial rise of structure A in hard X-rays is simultaneous with the rise of the 90 GHz profile to within the 128 ms resolution of the X-ray observations. The overall X-ray and 90 GHz time profiles appear slightly different, however.

In order to show these rapid mm-wave fluctuations more clearly, the gradually varying component of the 90 and 30 GHz flux has been removed in the plots shown in Figure 3 by subtracting a running mean. Plots for the three major structures A, B and C are shown together with a similar plot for a 4 s interval prior to the burst. Note that the system noise amplitude is negligible compared to the pulse sizes.

It is clear from Figure 3 that the rapid fluctuations in structure A are evident only at 90 GHz. The pulse repetition rate is ~ 5 Hz but a Fourier analysis¹⁶ shows that there is significant power at frequencies extending from 1 to 8 Hz. The relative amplitudes of the pulses range from 30 to 50% of the mean flux. Such pulses are barely noticeable at 30 GHz, however, and they have much smaller amplitude. The situation for structure B is somewhat different with pulse trains evident at both 90 and 30 GHz. The five pulses observed in approximately one second starting at 13^h26^m43^s UT are essentially in phase at the two frequencies but the relative amplitudes are still much larger at 90 GHz (60%) than at 30 GHz (1%). Structure C in Figure 3 also shows a train of pulses but with lower relative amplitude at both frequencies.

The pulse trains at 30 GHz with relative amplitudes of $< 1\%$ are comparable to the ultra fast structures observed for other bursts at 22 and 44 GHz^{17,18}. Similar subsecond pulses have been detected in hard X-rays in coincidence with microwave pulse at these same frequencies¹⁹ but the relative amplitudes of the hard X-ray pulses were 30 - 40%, comparable to the amplitudes of the 90 GHz pulses reported here.

The apparent brightness temperature of the burst source at mm-waves can be estimated if some assumptions are made for the velocity scales involved at the pulses acceleration site. If we assume the speed of light as a limit, the scale sizes for the 30 ms rise times becomes $L < 9 \times 10^8$ cm (or apparent size $\theta_s < 13$ arcsec). If we assume Alfvén speeds (10^8 cm s⁻¹), we obtain $L < 3 \times 10^6$ cm (or $\theta_s < 0.04$ arcsec). The apparent brightness temperature T_B is related to the excess antenna noise temperature T_A by the well known relationship $T_B \approx T_A (\theta_A/\theta_s)^2$, where θ_A is the antenna beamwidth. For structure A pulses we obtained antenna temperatures of 2500K at 90 GHz and 1400K at 30 GHz. With $\theta_A = 80$ arcsec at 90 GHz and $\theta_A = 3$ arcmin at 30 GHz, we obtain comparable apparent brightness temperatures at both frequencies of about 10^5 K (speed of light) and 10^{10} K (Alfvén speed), respectively.

The class of solar burst emitting at the shortest mm-wavelengths brings important constraints to existing models for explaining the geometry and mechanisms of particle accelerations in the impulsive phase. Further investigations at > 90 GHz are required in order to determine the turnover frequency of this new spectral component of burst emission.

We acknowledge the help received in Itapetinga observations from R.E. Schaal, J.L. Horner and R.H. Trevisan. The assistance of Shelby Kennard in the analysis of the HXRBS data is also acknowledged. INPE operates CRAAM and the Itapetinga Radio Observatory. This research received partial support from the Brazilian research agency FINEP.

References

1. Coates, R.J., Proc. National Electronics Conf., XIII, 1-12 (1957).
2. Coates, R.J., Proc. IRE, 46, 122-126 (1958).
3. Croom, D.L. and Powell, R.J., Nature, 221, 945 (1969).
4. Croom, D.L., Solar Phys., 15, 414-423 (1970).
5. Cogdell, J.R., Solar Phys., 22, 147-149 (1972).
6. Feix, G., J. Geophys. Res., 75, 211-218 (1970).
7. Shimabukuro, F.I., Solar Phys., 15, 424-432 (1970).
8. Shimabukuro, F.I., Solar Phys., 23, 169-177 (1972).
9. Nakajima, H., Sekiguchi, H., Sawa, M., Kai, K., Kawashima, S., Kosugi, T., Shibuya, N., Shinohara, N. and Shiomi, Y., Publ. Astron. Soc. Japan, submitted (1984).
10. Magun, A., private communication (1984).
11. Kaufmann, P., Strauss, F.M., Schaal, R.E. and Laporte, C., Solar Phys., 78, 389 (1982).
12. Orwig, L.E., Frost, K.J. and Dennis, B.R., Solar Phys., 65, 25 (1980).
13. Hertzberg Institute of Astrophysics, Solar Activity report for May 1984, NRC, Ottawa, Canada (1984).
14. Sagamore Hill Radio Observatory, U.S. Air Force.
15. Kiplinger, A.L., Dennis, B.R., Emslie, A.G., Frost, K.J., and Orwig, L.E., Ap.J. Letters, 265, L99 (1983).
16. Brenner, N., in Astrophysics, Part C: Radio Observations (Methods of Experimental Physics) (Ed. by M.L. Meeks), Academic Press, New York, vol 12, p. 284 (1976).
17. Kaufmann, P., Strauss, F.M., Opher, R. and Laporte, C., Astron. Astrophys., 87, 58 (1980).
18. Kaufmann, P., Correia, E., Costa, J.E.R., Dennis, B.R., Hurford, G.J. and Brown, J.C., Solar Phys., in press (1984).
19. Takakura, T., Kaufmann, P., Costa, J.E.R., Degaonkar, S.S., Ohki, K. and Nitta, N., Nature, 302, 317 (1983).

FIGURE CAPTIONS

Figure 1. The solar burst on 1984 May 21 at 13^h26^m UT as observed by HXRBS in X-rays at 24 - 108 keV and 108 - 219 keV, and in mm/cm waves at 90, 30 and 7 GHz. The s.f.u. scale is subject to an uncertainty of a factor of < 2. Major structures in the time profiles labelled A, B, and C are discussed in the text and are plotted on expanded time scales in Figures 2 and 3.

Figure 2. 4s expansion of the 24 - 440 keV X-ray and 90 GHz intensities in structure A of the burst shown in Figure 1. The vertical bars on the X-ray plot indicate $\pm 1 \sigma$ uncertainties in the measured rate based on the square-root of the observed number of counts in each interval. The horizontal bars indicate the 128ms time intervals over which the counting rates, corrected for instrumental dead time, were determined. The time constant used for the 90 GHz plot was 10ms and the system noise was comparable to the thickness of the line.

Figure 3. Major burst structures at 90 and 30 GHz, labelled A, B, and C in Figure 1, plotted on an expanded time scale with a running mean subtracted from the measured fluxes. The flux variations in a 4s interval are plotted for each structure at the two frequencies with a similar plot at the top of the figure showing the system noise in a 4s interval one minute before the start of the burst. The vertical scale for the 90 GHz plots is the same for all four intervals and is given to the left of the curves for structure A. Similarly, the common scale for the 30 GHz plots is given to the left of the curves for structure B.

ORIGIN UNKNOWN
OF POOR QUALITY

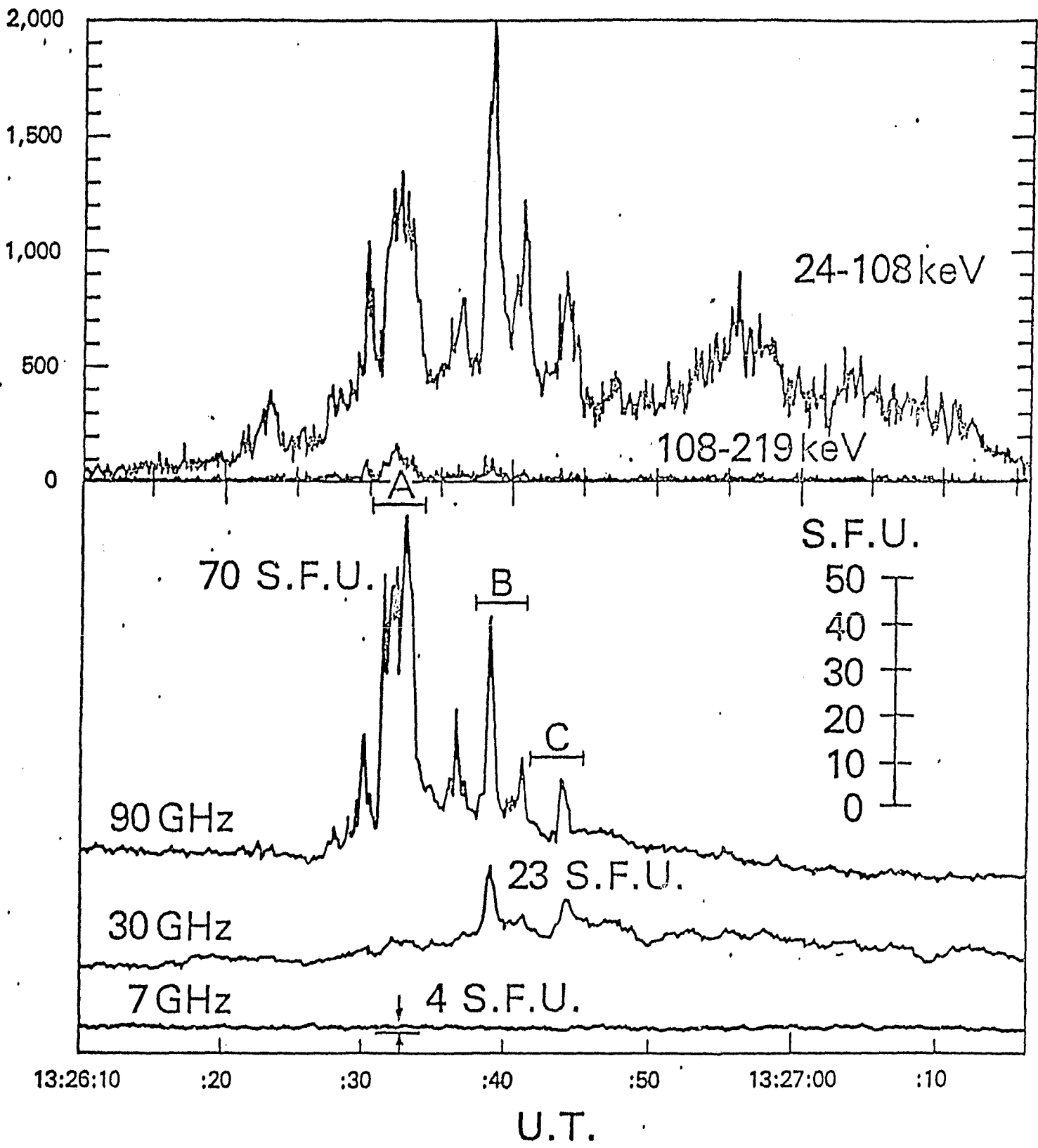


Figure 1

ORIGINAL PAGE IS
OF POOR QUALITY

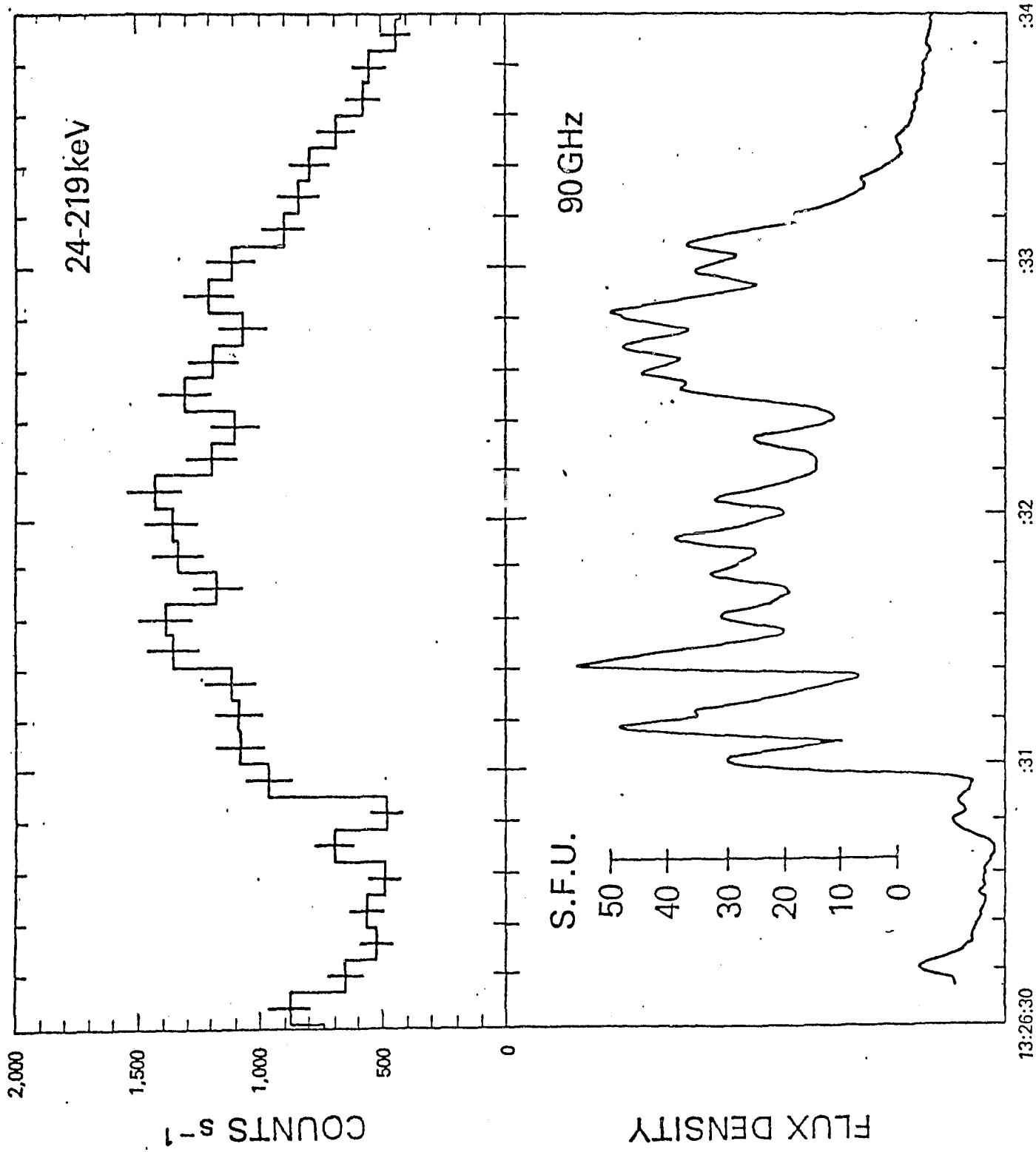


Figure 2

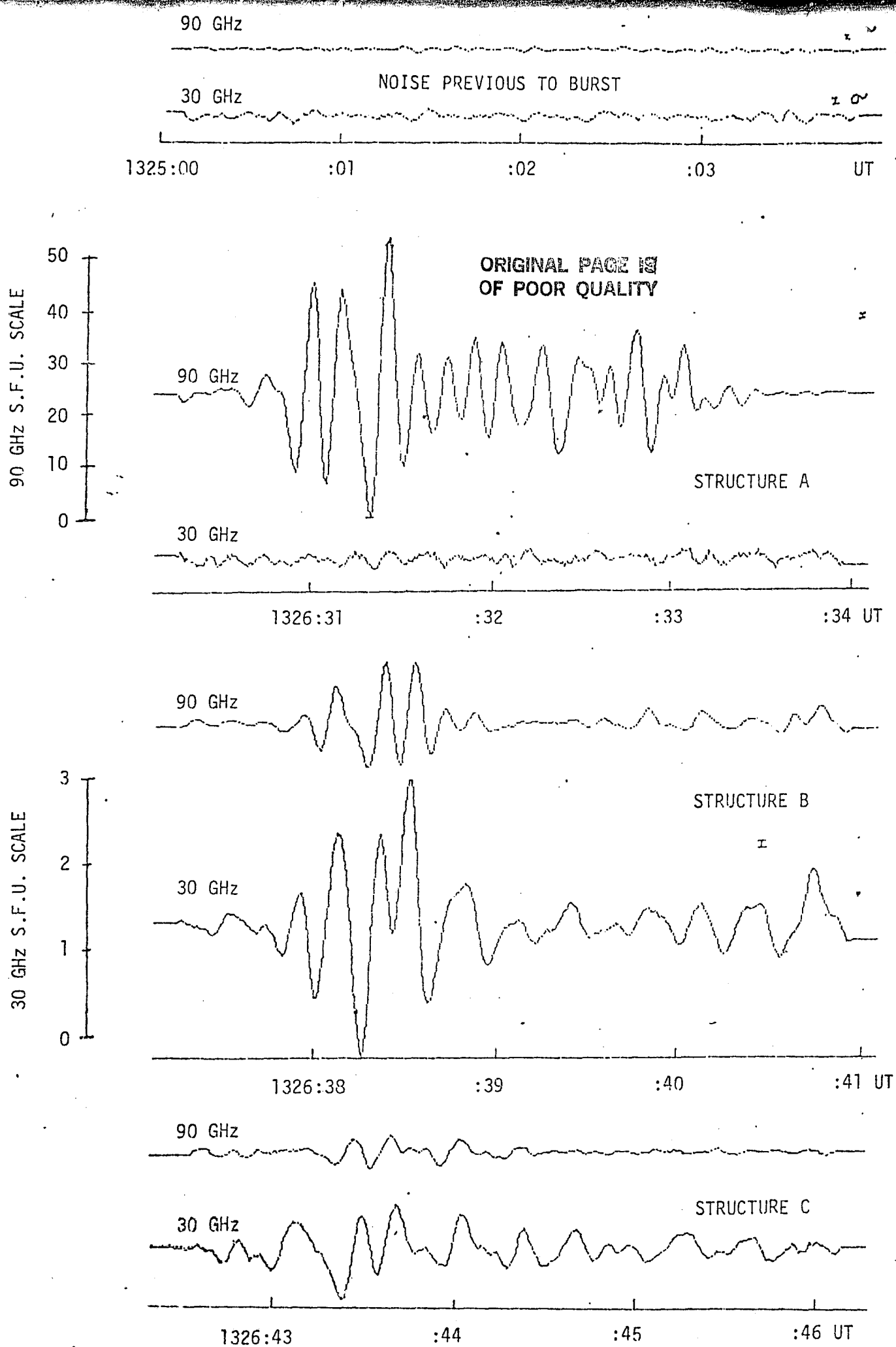


FIG. 3